

ESCAPE OF IONIZING RADIATION FROM STAR FORMING REGIONS IN YOUNG GALAXIES

ALEXEI O. RAZOUMOV¹ AND JESPER SOMMER-LARSEN²

Draft version February 26, 2018

ABSTRACT

Using results from high-resolution galaxy formation simulations in a standard Λ CDM cosmology and a fully conservative multi-resolution radiative transfer code around point sources, we compute the energy-dependent escape fraction f_{esc} of ionizing photons from a large number of star forming regions in two galaxies at five different redshifts from $z = 3.8$ to 2.39 . All escape fractions show a monotonic decline with time, from (at the Lyman-limit) $\sim 6 - 10\%$ at $z = 3.6$ to $\sim 1 - 2\%$ at $z = 2.39$, due to higher gas clumping at lower redshifts. It appears that increased feedback can lead to higher f_{esc} at $z \gtrsim 3.4$ via evacuation of gas from the vicinity of star forming regions and to lower f_{esc} at $z \lesssim 2.39$ through accumulation of swept-up shells in denser environments. Our results agree well with the observational findings of Inoue et al. (2006) on redshift evolution of f_{esc} in the redshift interval $z = 2 - 3.6$.

Subject headings: galaxies: formation — intergalactic medium — HII regions — radiative transfer

1. INTRODUCTION

In the redshift interval $2 < z < 6$ most ionizing photons in the Universe are thought to originate in PopII stars in normal ($V_c \gtrsim 30 - 50 \text{ km s}^{-1}$) galaxies (Nagamine et al. 2006). For reionization calculations at $z > 6$ photons from lower mass halos should be taken into account (Iliev et al. 2006), whereas at $z \sim 2$ active galactic nuclei start to play a dominant role (Madau et al. 1999). The fact that the metagalactic UV field peaks at $2 < z < 4$ (Inoue et al. 2006, and ref. therein) points to a peak in the galactic star formation (SF) rate at such redshifts (see also Panter et al. 2006). A major uncertainty in modeling the effect of this SF on the thermal state of the intergalactic medium (IGM) is the value of the escape fraction f_{esc} of ionizing UV photons, which is a function of redshift, and galaxy type and mass.

Best observational estimates of f_{esc} come from the detailed multiwaveband studies of the local Universe. Leitherer et al. (1995) find that less than 3% of ionizing photons from low-redshift starburst galaxies escape into the IGM. More recently, for several local starburst galaxies, Heckman et al. (2001) estimate $f_{\text{esc}} \lesssim 6\%$, noting that inclusion of dust will further reduce f_{esc} , and Bergvall et al. (2006) find $f_{\text{esc}} \sim 4 - 10\%$ for another local starburst.

The situation is markedly different at $z \gtrsim 3$, where the Lyman continuum (LyC) detection points at much higher f_{esc} (Steidel et al. 2001). By comparing the direct observations of the LyC from galaxies to the mean cosmic UVB intensity, Inoue et al. (2006) conclude that the average f_{esc} increases from $1 - 2\%$ at $z = 2$ to $\sim 10\%$ at $z \gtrsim 3.6$.

Most theoretical estimates of f_{esc} to date have been based on models with a smooth distribution of gas

(Ricotti & Shull 2000) or semi-analytical models with expanding shells and superbubbles in a disk galaxy (Dove et al. 2000; Fujita et al. 2003). In this letter we present ab initio calculations of the energy-dependent f_{esc} of ionizing radiation from SF regions in protogalaxies found in numerical simulations at five different redshifts from $z = 2.39$ to 3.8 . We define $f_{\text{esc}}(\nu, r)$ simply as a fraction of photons of energy $h\nu$ which reach a shell of radius r around a given source; by definition $f_{\text{esc}}(\nu, 0) = 1$. We postprocess high-resolution simulation datasets with radiative transfer (RT) on nested grids, with the maximum grid resolution of 15 pc. Each galaxy contains from several hundred to several thousand distinct stellar sources representing individual, young SF regions. Our interstellar gas distribution is extremely clumpy due to an array of physical processes including feedback from SF. We also estimate the effect of the dynamical expansion of HII regions on the escape of ionizing photons.

2. THE CODE AND MODELS

To compute the escape of ionizing radiation from SF regions, we use an extension of the Fully Threaded Transport Engine (FTTE, Razoumov & Cardall 2005) to point sources. This new module was previously briefly introduced in the comparison study by Iliev et al. (2006). It extends the adaptive ray-splitting scheme of Abel & Wandelt (2002) to a model with variable grid resolution. Sources of radiation can be hosted by cells of any level of refinement, although usually in cosmological applications sources are sitting on the deepest level of refinement (Fig. 1). Around each point source we build a system of $12 \times 4^{n-1}$ radial rays which split either when we move further away from the source, or when we enter a refined cell, and $n = 1, 2, \dots$ is the angular resolution level. Once a radial ray is refined it stays refined, even if we leave the high spatial resolution patch, until even further angular refinement is necessary. All ray segments are stored as elements of their host cells, and for actual transport we just follow these interconnected data structures accumulating photo-reaction number and energy rates in each cell. With multiple sources, we add the rates from

Electronic address: razoumov@ap.smu.ca
Electronic address: jslarsen@dark-cosmology.dk

¹ Institute for Computational Astrophysics, Dept. of Astronomy & Physics, Saint Mary's University, Halifax, NS, B3H 3C3, Canada

² Dark Cosmology Centre, Niels Bohr Institute, University of Copenhagen, Juliane Maries Vej 30, DK-2100 Copenhagen, Denmark

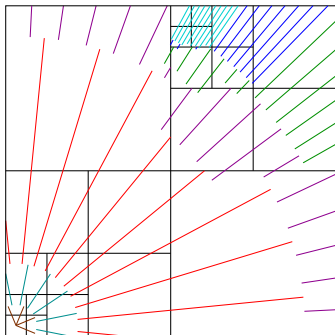


FIG. 1.— Radial ray geometry in the FTTE point source algorithm. Color represents the angular resolution level. To avoid a non-uniform coverage of a cell such as that seen at the top of this box, we normally avoid cell interfaces with a jump in refinement by more than one level.

all sources before updating the time-dependent rate network using the chemistry solver from Abel et al. (1997), and the global timestep is chosen such that each species abundance does not change by more than 30%.

With a small ($N_{\text{src}} < 10^3$) number of star particles we can compute a full ray geometry separately for each source. For a large number of sources ($10^3 - 10^6$) the algorithm allows construction of trees of sources in which individual tree nodes are treated as a single source far from their origin.

Our algorithm shares many common ideas with the recent RT module of the cosmological structure formation code Enzo implemented by Abel et al. (2006) to study feedback from Pop III stars and, in fact, is a basis of an independently developed radiation hydrodynamics module of Enzo which we will introduce elsewhere.

2.1. Galaxy formation models

We use results of high-resolution galaxy formation simulations in a standard Λ CDM cosmology done with a significantly improved version of the TreeSPH code described by Sommer-Larsen et al. (2003) – some detail is given in Sommer-Larsen (2006). The simulations invoke the formation of discrete star “particles”, which represent a population of stars born at the same time in accordance with a given initial mass function (IMF). For the purpose of this work we focus on two (proto-) galaxies, K15 and K33, which at $z=0$ become typical disk galaxies of $V_c = 245$ and 180 km s^{-1} , respectively. The RT calculation are performed at five different redshifts, $z = 3.8, 3.6, 3.4, 2.95$, and 2.39 , for “normal” resolution simulations, and at the first three for “high” resolution ones (8 times higher mass resolution, twice better force resolution). For galaxy K15 we also vary the strength of supernova feedback (Table 1). Total particle numbers range from $\sim 1.6 \times 10^5$ to $\sim 2.2 \times 10^6$; star (and SPH) particle masses are 1.1×10^6 and $1.4 \times 10^5 M_{\odot}$, for normal and high resolution simulations, respectively.

Radiative transfer is computed on top of a nested data structure containing 3D distributions of physical variables. To create such a structure from the SPH simulation datasets, for each galaxy we cut out a $(250 \text{ kpc})^3$ box centered on the galaxy and projected this box onto a 128^3 uniform grid. We then subdivided every base grid cell which contains more than $N_{\text{max}} = 10$ SPH particles,

TABLE 1
NUMBER OF DISTINCT STAR-PARTICLES OF AGE ≤ 34 MYR.

Simulation	resolution	feedback	$z=3.8$	3.6	3.4	2.95	2.39
galaxy 1							
K15-1-8	normal	>normal		347		1000	560
K15-06-8	normal	normal	431	560	595	1161	596
K15-06-64	high	normal	5061	5248	6005		
galaxy 2							
K33-06-8	normal	normal	306	340	390	337	144
K33-06-64	high	normal	2566	3122	3389		

and continued this process of subdivision recursively so that no cell contains more than N_{max} gas particles.

2.2. Stellar population synthesis

In the (normal resolution) galaxy K15-1-8 at $z = 3.6$ there are 347 stellar sources younger than $t_{\text{up}} = 34 \text{ Myrs}$ (Fig. 2). The birth times of particles are distributed almost uniformly over the span of 34 Myrs, corresponding to a nearly constant star formation rate (SFR) of $11.6 M_{\odot}/\text{yr}$. To compute the stellar UV luminosity function for this and other galaxies, we use a population synthesis package Starburst 1999 (Leitherer et al. 1999) with continuous SF at a constant rate $11.6 M_{\odot}/\text{yr}$ distributed among 347 stars. For other galaxies and at other redshifts the SFR per particle is adjusted to account for the actual number of stars produced in the past 34 Myrs, and the specific (per unit spectrum) luminosity is distributed uniformly among all stars in the volume.

We assume a triple-interval Kroupa IMF with indices (0.5, 1.2, 1.7) above the mass boundaries (0.1, 0.5, 1) M_{\odot} , respectively, a supernova cut-off at $8 M_{\odot}$, a black hole cut-off $120 M_{\odot}$, and solar metallicity. The resulting spectrum is shown in the lower right panel of Fig. 2.

2.3. Heating and HII region expansion

The TreeSPH code assumes the UVB of Haardt & Madau (1996) with self-shielding in regions in which the mean free path of Lyman-limit photons is less than 1 kpc. In addition to radiative heating and cooling and the hydrodynamical PdV term, some heating originates from shock dissipation which we include in the following way. After we project the 3D hydro fields onto the grids, in each cell we apply the uniform UVB with the self-shielding correction and compute the amount of additional heating needed to keep the temperature of that cell constant (thermal equilibrium without sources). We then switch on the stellar sources retaining the extra heating term, and evolve simultaneously the equations of point source transfer and non-equilibrium chemistry to 10 Myrs. With continuous SF and constant UV luminosities, all f_{esc} reach a plateau after the first few Myrs. In this paper all results are presented at $t = 10 \text{ Myrs}$ at which point we assume convergence.

Direct momentum transfer from UV photons to the interstellar/intergalactic gas is negligible (Spitzer 1978; Whalen & Norman 2006). However, heating and ionization by stellar photons creates pressure gradients that drive expansion of the HII regions into the surrounding gas. The physics of expansion has been studied in detail in 1D (Kitayama et al. 2004; Whalen & Norman 2006),

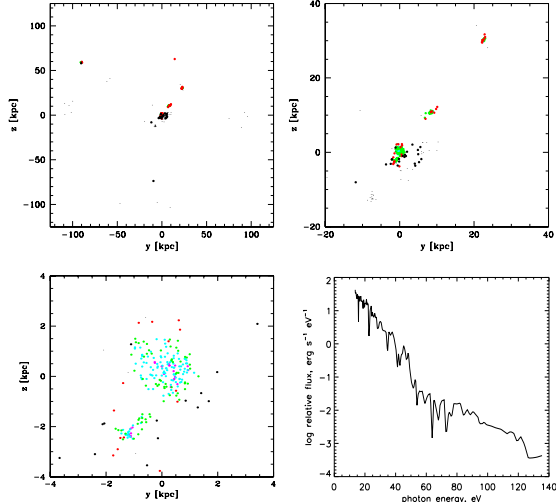


FIG. 2.— The distribution of all stellar particles (SF regions) younger than $t_{\text{up}} = 34$ Myrs in the volumes 250 kpc (top left), 60 kpc (top right) and 8 kpc (lower left) on a side centered on the galaxy K15-1-8 at $z = 3.6$. The color of each particle represents the level of the host cell: purple circles (level 5), light blue circles (level 4), green circles (level 3), red circles (level 2), black circles (level 1), and black dots (base grid level 0 cells). The lower right panel shows the input spectrum of a star particle.

2D (Shapiro et al. 2004), and recently 3D (Abel et al. 2006) radiation hydrodynamics simulations. Without coupling RT to the hydro code, we cannot model this expansion self-consistently. However, we can mimic its effect by lowering the density in the giant HII region around the starburst region which will ease the escape of UV photons. We use the results from section 3.1 of Larsen et al. (2001) which lists the "initial Strömgren radius" R_0 (1 Myr after the burst) and the "final Strömgren sphere" R_e (4 Myr after the burst; at this time the UV luminosity declines rapidly) as a function of the local density and the ionizing source luminosity.

For each source we use the initial gas density n_0^{src} of the its host cell to find R_0 and R_e and then modify the density of each cell inside R_e by $n_e^{\text{src}}/n_0^{\text{src}}$, provided that the initial density of that cell $n_0 \leq n_0^{\text{src}}$. For $n_0 > n_0^{\text{src}}$ the expanding shell hits a denser region, and without a full hydrodynamical calculation one cannot predict whether this will lead to expansion or compression of the denser region, which explains our condition. Therefore, for a given source our density correction is anisotropic which seems entirely realistic for an HII front expansion in an inhomogeneous medium.

For such large galaxies, we do not expect our results to change significantly if a fully self-consistent hydro/RT approach is used, as the energetic and momentum effects of ionization fronts are negligible compared to the effects of SNII explosions, shocks etc. which are already included into our models, resulting in a very clumpy interstellar medium (ISM). However, the radiative feedback would also smooth some of the small-scale structure by raising the Jeans mass which is especially important in lower mass galaxies, an effect which we plan to include in our future simulations.

3. RESULTS AND DISCUSSION

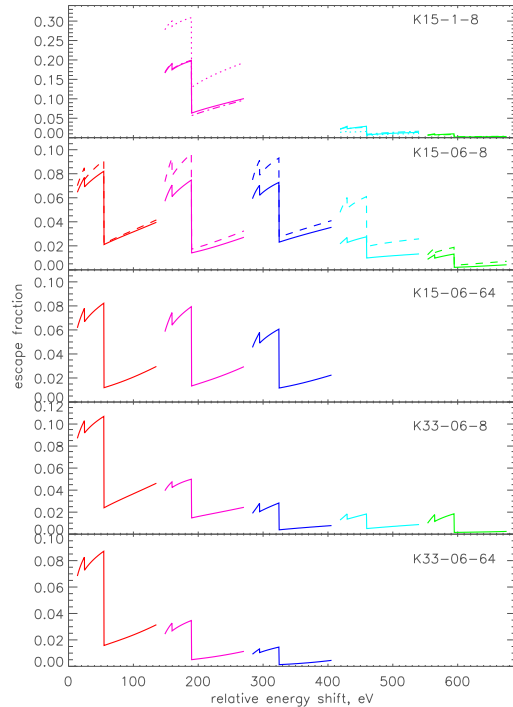


FIG. 3.— Spectral dependence of f_{esc} at $r = 100$ kpc for all five input galaxy models at (where transfer has been computed) $z = 3.8$ (red), $z = 3.6$ (magenta), $z = 3.4$ (blue), $z = 2.95$ (cyan), and $z = 2.39$ (green). For each model the redshift evolution is from left to right, and each curve goes from 13.6 eV to 135 eV. All solid lines are models without the HII region expansion, with the SFR distributed uniformly among all stars younger than 34 Myrs. For K15-06-8 the dashed lines show models with the HII region expansion. For K15-1-8 we also computed the models with the *same* SFR distributed among stars younger 3.4 Myrs (dotted) and 10 Myrs (dash-dotted lines).

Fig. 3 shows spectral dependence of f_{esc} at $r = 100$ kpc in each model, averaged over all sources. All f_{esc} have been corrected for the boundary of the volume. For individual sources the escape of photoionizing radiation is similar to a phase transition: it is very sensitive to conditions at the source and therefore can vary by a sizable factor for the same galaxy over the course of its evolution. We find that while there are variations among the models, the escape fractions tend to decrease with lower redshift, reflecting the fact that with time more gas cools into the higher density clouds, as well the declining SFR at $z < 2.95$. With normal feedback in both galaxies f_{esc} at the Lyman edge drops from 8 – 10% at $z = 3.8$ to $\sim 1 - 2\%$ at $z = 2.39$.

Not surprisingly, in all our models f_{esc} of photons capable of doubly ionizing helium is very low, due to the softness of stellar radiation. The escape fraction of photons capable of single He ionization is comparable at all redshifts to that of H-ionizing photons.

Increasing SN feedback in K15 evacuates more gas from the vicinity of the SF regions leading to a threefold rise in f_{esc} at $z = 3.6$. Lower local gas densities translate into a 40% reduction in the SFR (Table 1). At $z = 2.95$, a denser environment near the sources produces a much smaller difference in the SFR and f_{esc} , when we increase the strength of feedback, and, at $z = 2.39$, f_{esc} actually

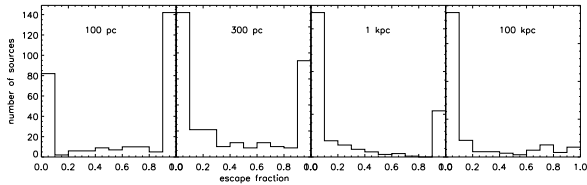


FIG. 4.— Lyman-limit escape fraction distribution for all sources in galaxy K15-1-8 at $z = 3.6$ (without HII region expansion), at four different radii, from 100 pc to 100 kpc.

drops by 25% as a larger fraction of gas swept-up by the shocks stays in the vicinity of the SF regions.

Next we compare our normal and high resolution results, at $z = 3.8-3.4$, and find a good agreement between the two. We see it as an additional test of our algorithm, since other properties of the two sets of simulations (SFR, etc.) also match.

Since our choice of distributing SF over the $t_{\text{up}} = 34$ Myrs youngest stars is somewhat arbitrary, in galaxy K15-1-8 we also experimented with the same amount of SF distributed over all stars younger than $t_{\text{up}} = 10$ Myrs and 3.4 Myrs. Ideally, these young stars would produce most of the ionizing UV photons. Since we do not calculate transfer and hydro simultaneously, we feel that applying continuous SF with the constant rate is a better computational approach than assuming instantaneous SF which will have no lasting effect on the thermal state of the IGM after few Myrs. With continuous SF we expect our results to converge as we increase the number of star particles. The results at $t_{\text{up}} = 10$ Myrs and 34 Myrs are in fact very close to each other at all three redshifts (Fig. 3), whereas the 3.4 Myrs results are somewhat off, likely related to the small number of sources used to represent the SF in this latter case.

The dashed lines in K15-06-8 in Fig. 3 show the energy-dependent f_{esc} at $r = 100$ kpc corrected for the HII region expansion. At most redshifts expansion raises f_{esc} by 10–30%, although at $z = 2.95$ f_{esc} jumps by more than a factor of two. Further analysis shows that most of this change can be attributed to removal of the gas from the highest refinement level cells which are hosting the sources, not the surrounding cells.

In Fig. 4 we show how f_{esc} changes with distance from sources in galaxy K15-1-8 at $z = 3.6$. A large fraction of photons reaches the radius $r = 100$ pc. As we do not

have any reliable information on gas clumping on sub-resolution scales at these redshifts, the effective radius of absorption is not firmly established at this point. In our current models most absorption occurs within few hundreds pc of each star particle, well inside the virial radius of ~ 45 kpc. At $z = 3.6$, the proto-galaxy consists of several star forming regions as well as a significant amount of the intergalactic HI, all of which account for some fractional absorption beyond 1 kpc.

In this study we neglected the effect of dust extinction. Benson et al. (2006) point out that in the case of a smooth ISM attenuation by dust can reduce f_{esc} by a factor of few. For a clumpy ISM at high redshifts the magnitude of dust attenuation should be much lower, particularly that most ionizing photons are produced in star bursts, as opposed to a quiescent disk.

In conclusion, our models with exact ionizing continuum RT around a large number of SF regions in young protogalaxies show a monotonic decline in f_{esc} of ionizing photons from higher to lower redshifts. With the normal feedback strength f_{esc} at the Lyman edge drops from $\sim 6-10\%$ at $z = 3.6$ to $\sim 1-2\%$ at $z = 2.39$. At higher redshifts SF on average occurs at slightly lower densities resulting in easier escape of UV photons into the IGM. This result agrees well with the observational findings of Inoue et al. (2006) on redshift evolution of f_{esc} . Note that although the two galaxies in our study have a mass ratio of ~ 2.5 , their f_{esc} are very similar. One could suggest that perhaps, once star formation begins, it is the physical conditions in the clumpy gas clouds that determine the escape of UV photons, rather than the overall properties of their host galaxies. However, one would need a much larger statistical sample to test this speculation. In our next paper we will further examine the role of the fine structure of the clumpy ISM in the escape of ionizing photons, as well as the importance of hydrodynamical effects.

AR would like to thank Mika Juvela and Eric Lentz for valuable discussions on numerical methods, as well as the hospitality of the Dark Cosmology Centre at the University of Copenhagen. The TreeSPH simulations were performed on the SGI Itanium II facility provided by DCSC. The Dark Cosmology Centre is funded by the DNRF.

REFERENCES

- Abel, T., Anninos, P., Zhang, Y., & Norman, M. L. 1997, *New Astronomy*, 2, 181
- Abel, T. & Wandelt, B. D. 2002, *MNRAS*, 330, L53
- Abel, T., Wise, J. H., & Bryan, G. L. 2006, *astro-ph/0606019*
- Benson, A. J., Sugiyama, N., Nusser, A., & Lacey, C. G. 2006, *MNRAS*, 369, 1055
- Bergvall, N., Zackrisson, E., Andersson, B.-G., Arnberg, D., Masegosa, J., & Östlin, G. 2006, *A&A*, 448, 513
- Dove, J. B., Shull, J. M., & Ferrara, A. 2000, *ApJ*, 531, 846
- Fujita, A., Martin, C. L., Mac Low, M.-M., & Abel, T. 2003, *ApJ*, 599, 50
- Heckman, T. M., Sembach, K. R., Meurer, G. R., Leitherer, C., Calzetti, D., & Martin, C. L. 2001, *ApJ*, 558, 56
- Iliev, I. T., Ciardi, B., Alvarez, M. A., Maselli, A., Ferrara, A., Gnedin, N. Y., Mellema, G., Nakamoto, T., Norman, M. L., Razoumov, A. O., Rijkhorst, E.-J., Ritzerveld, J., Shapiro, P. R., Susa, H., Umemura, M., & Whalen, D. J. 2006, *MNRAS*, 873
- Iliev, I. T., Mellema, G., Shapiro, P. R., & Pen, U.-L. 2006, *astro-ph/0607517*
- Inoue, A. K., Iwata, I., & Deharveng, J.-M. 2006, *MNRAS*, 371, L1
- Kitayama, T., Yoshida, N., Susa, H., & Umemura, M. 2004, *ApJ*, 613, 631
- Larsen, T. I., Sommer-Larsen, J., & Pagel, B. E. J. 2001, *MNRAS*, 323, 555
- Leitherer, C., Ferguson, H. C., Heckman, T. M., & Lowenthal, J. D. 1995, *ApJ*, 454, L19
- Leitherer, C., Schaerer, D., Goldader, J. D., Delgado, R. M. G., Robert, C., Kune, D. F., de Mello, D. F., Devost, D., & Heckman, T. M. 1999, *ApJS*, 123, 3
- Madau, P., Haardt, F., & Rees, M. J. 1999, *ApJ*, 514, 648
- Nagamine, K., Cen, R., Furlanetto, S. R., Hernquist, L., Night, C., Ostriker, J. P., & Ouchi, M. 2006, *New Astronomy Review*, 50, 29

- Panter, B., Jimenez, R., Heavens, A. F., & Charlot, S. 2006, astro-ph/0608531
- Razoumov, A. O. & Cardall, C. Y. 2005, MNRAS, 362, 1413
- Ricotti, M. & Shull, J. M. 2000, ApJ, 542, 548
- Shapiro, P. R., Iliev, I. T., & Raga, A. C. 2004, MNRAS, 348, 753
- Sommer-Larsen, J. 2006, ApJ, 644, L1
- Sommer-Larsen, J., Götz, M., & Portinari, L. 2003, ApJ, 596, 47
- Spitzer, L. 1978, Physical processes in the interstellar medium (New York Wiley-Interscience, 1978. 333 p.)
- Steidel, C. C., Pettini, M., & Adelberger, K. L. 2001, ApJ, 546, 665
- Whalen, D. & Norman, M. L. 2006, ApJS, 162, 281